A beginners guide to fundamental experiments in quantum optics using the Thorlabs Quantum Optics Educational Kit

Student name: Kshitij

Supervisor: Prof. Maksim Skorobogatiy

Contents

1 Introduction

With a strong interest in experimental quantum optics, I joined Prof. Maksim Skorobogatiy's lab at Polytechnique Montréal, Canada via the MITACS Globalink Graduate Fellowship program in the summer of 2024. After my introduction to the lab, I was tasked with performing the fundamental quantum optic experiments using the Thorlabs Quantum Optics Educational Kit. There were several goals behind this activity including learning theoretical and experimental concepts of quantum optics, setting up and debugging the experimental system and learning its limitations, performing critical analysis of the results, and finally educating the group members in the basics of quantum optics via a series of workshops based on live experimental demonstrations and discussions.

During my work, I faced various challenges related to theoretical understanding and experimental demonstration of quantum optic phenomena. This pushed me into digging into the classical literature on the subject, as well as into technical manuals of many components used in the experiements. My progression into the project along with the observations and frustrations were condensed into the weekly reports which became the basis for the in-depth discussions with Prof. Skorobogatiy. On the experimental side, I faced a large number of difficulties in making things work and had to go through much trial and error. I went back and forth with Thorlabs Technical Support, who were very helpful in resolving the issues. With much persistence, I completed the six key experiments of quantum optics over the summer of 2024. These experiments are fundamental for anyone wanting to get into quantum optics and provide a great stepstone to understanding of the critical concepts involved.

The main motivation for this document is, therefore, to provide a practical guide for the beginners in experimental quantum optics, to save the frustration and make the learning process more streamlined for the beginners in the field. I consider this document as an addendum to an already excellent Thorlab's manual for the Quantum Optics Kit where I share my observations, interpretations and finer points of the functioning and arrangement of the experimental setups learned through hands-on experience.

I thank Prof. Maksim Skorobogatiy for hosting me in his lab, giving me this project, having in-depth intellectual and technical discussions related to quantum optics, as well as encouraging me to write this document highlighting my experiences. I would also like to thank his PhD student Vladislav Ulitko for assisting me during the internship, as well as Thorlabs Technical Support for helping in resolving many issues related to the kit. The software used for the experiments [1] was distributed by "Thorlabs, Inc.", which can be downloaded from their website or the pen drive in the kit and all the components used for the experiments are manufactured by "Thorlabs, Inc." and are part of the Thorlabs Quantum Optics Educational Kit.

2 Experiment 1 (HBT with Attenuated Laser)

Aim: Test whether an attenuated laser can serve as a single-photon source.

2.1 Theory

Hanbury Brown and Twiss (HBT) [2] experiment differentiates between classical and non-classical light sources. For this experiment, a light source is passed through a beamsplitter, incident onto two different single-photon detectors. The setup measures the count rates of both detectors and their coincidence count rates, which are then used to calculate a function called the second-order correlation function with a delay of 0, i.e., $g^{(2)}(0)$.

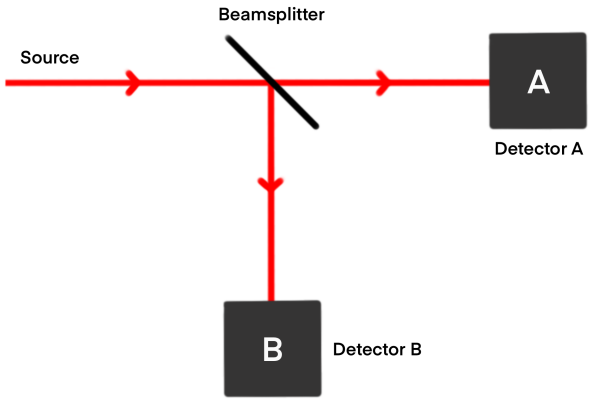

Figure 2.1: Schematic of simple HBT setup [3]

$$g^{(2)}_{HBT}(0) = \frac{R_{AB}}{R_A \cdot R_B \cdot \Delta t} \tag{1}$$

Where,
R_A and R_B are the average count rates of detectors A and B.
R_{AB} is the average count rate of coincidences.
Δt is the time window or coincidence interval.

The calculated $g^{(2)}(0)$ classifies the type of source [3],

$$g^{(2)}_{HBT}(0) > 1 \quad \text{implies classical.}$$
$$g^{(2)}_{HBT}(0) = 1 \quad \text{implies coherent.}$$
$$g^{(2)}_{HBT}(0) < 1 \quad \text{implies non-classical.}$$

2.1.1 Coincidence Counting

Let's first understand what any of this even means. A coincidence is counted when one detector detects a photon, and within a particular time window (Δt), the other detector detects another photon.

It is counted using the single-photon detectors and the time tagger. When many photons are incoming, defining a proper detection scheme becomes necessary.

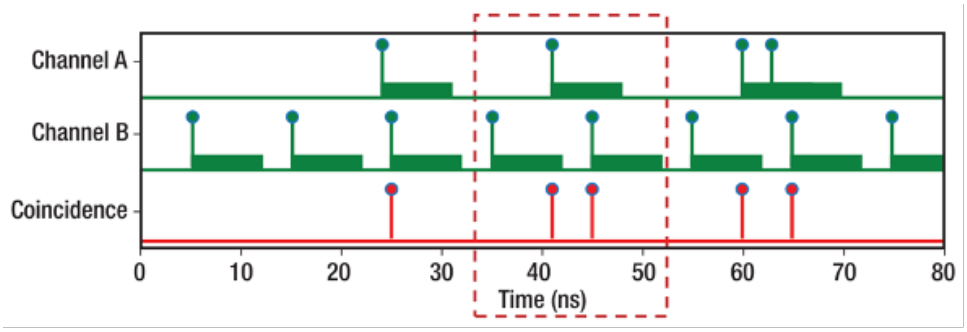

Figure 2.2: Coincidence scheme (Retrieved from: [3] Figure 19)

Here, bars indicate the length of the coincidence window, and the dashed rectangle highlights the undesired scenario where only one event in channel A results in two coincidences. This approach might appear unsuitable for quantum optics applications as a single detection event could cause multiple coincidence events, leading to over-counting. However, the dead time of the detectors prevents this scenario, which is much longer than the coincidence window. Therefore, the time tagger's definition of coincidences is appropriate for the experiments in the kit [3].

2.1.2 Second-Order Correlation Function ($g^{(2)}(0)$)

Consider the setup similar to the one in fig. 2.1 but with an added delay on the detector B side. For classical electromagnetic waves, the second-order correlation function [3] at a delay τ is given by:

$$g^{(2)}(\tau) = \frac{\langle I_A(t) \cdot I_B(t+\tau) \rangle}{\langle I_A(t) \rangle \cdot \langle I_B(t+\tau) \rangle} \tag{2}$$

Where, $I_A(t)$ and $I_B(t+\tau)$ are the intensities at detector A at the time t and at detector B at the time $t+\tau$, respectively. Delay is induced in an optical system by varying the path difference between the two sides. We consider the case where both the path lengths after the beamsplitter to the detector are the same, i.e., $\tau = 0$. We get,

$$g^{(2)}(0) = \frac{\langle I_A(t) \cdot I_B(t) \rangle}{\langle I_A(t) \rangle \cdot \langle I_B(t) \rangle} \tag{3}$$

Using the property of classical sources and Cauchy-Schwarz inequality, one can show that $g^{(2)}(0) \geq 1$ if the source is classical.

Now, when we are using single-photon detectors instead of photodiodes, the $g^{(2)}(0)$ expression needs to be modified since when a single photon arrives at the beamsplitter, it either reflects or transmits with equal probability (for $50/50$ beamsplitter). Such measurements in quantum optics are done at very low intensities using single-photon detectors that output counts instead of a continuous signal. For this case, the count rate should be proportional to the intensity of the light.

With this in mind, the following probabilities are defined,

$$P_A = \eta_A \cdot \langle I_A(t) \rangle \cdot \delta t \tag{4}$$

$$P_B = \eta_B \cdot \langle I_B(t) \rangle \cdot \delta t \tag{5}$$

$$P_{AB} = \eta_A \cdot \eta_B \cdot \langle I_A(t) \cdot I_B(t) \rangle \cdot \delta t^2 \tag{6}$$

Where, P_A and P_B are probabilities of detecting photons at detectors A and B in a short time δt, respectively. P_{AB} is the probability of detecting photons simultaneously at one detector in a short time δt and at the other detector again in a short time δt. η_A and η_B are detection efficiencies of detectors A and B that are incident with light of intensities $I_A(t)$ and $I_B(t)$ respectively. Substituting in eq. 3 gives,

$$g^{(2)}(0) = \frac{P_{AB}}{P_A \cdot P_B} \tag{7}$$

The probability of coincidences P_{AB} could be expressed using the average count rate of coincidences R_{AB} by multiplying with the time window Δt. The probabilities P_A and P_B also could be similarly expressed using the average count rates R_A and R_B of the detectors A and B, respectively.

$$P_A = R_A \cdot \Delta t \qquad P_B = R_B \cdot \Delta t \qquad P_{AB} = R_{AB} \cdot \Delta t \tag{8}$$

Substituting in eq. 7, gives us the final form of $g^{(2)}(0)$ used in the kit,

$$g^{(2)}(0) = \frac{R_{AB}}{R_A \cdot R_B \cdot \Delta t} \tag{9}$$

Here, we can see that:

1. If the source is a coherent laser, $I_A(t) = I_B(t)$ for a $50:50$ beamsplitter. So, from eq. 3, $g^{(2)}(0) = 1$.

2. If the source is completely anti-correlated (quantum), then $P_{AB} = 0$ as at a particular time, a photon could either reflect or transmit and not both simultaneously. So, from eq. 7, $g^{(2)}(0) = 0$.

3. If the source is highly correlated, then the average coincidence intensity is higher than the average product of the individual intensities. So, from eq. 3, $g^{(2)}(0) > 1$.

For the kit, the $g^{(2)}_{HBT}(0)$ value is not simply $\tau = 0$, but rather, it is an integration of $g^{(2)}(\tau)$ for τ over the range of Δt centered around $\tau = 0$.
It means that while measuring thermal states, even though the value $g^{(2)}_{HBT}(0)$ should be 2 ideally, when we see around $\tau = 0$, the $g^{(2)}_{HBT}(\tau)$ value quickly drops down and stagnates at 1 [3]. It happens in a very small time scale in the order of femtoseconds, which is referred to as the coherence time of the light. But since Δt in the kit is if the order of nanoseconds, averaging over the range results in a value equal to 1.

2.1.3 Types of Light Sources and the First Problem Question

In the manual, light is described in three different states [3], Fock states, Coherent state, and Thermal states. Here,

Thermal states,	$g^{(2)}_{HBT}(0) = 2$	implies classical source.
Coherent states,	$g^{(2)}_{HBT}(0) = 1$	implies coherent source.
Fock states,	$g^{(2)}_{HBT}(0) = 0$	implies quantum source.

Laser sources are basically coherent sources, while single-photon sources are quantum sources. In the experiments performed in the kit, we only work with coherent and non-classical sources.

Now, if lasers are a barrage of photons, would it be considered a quantum source if we reduce its intensity a lot, leaving only a few photons?

2.2 Experimental Setup and Procedure

In fig. 2.3, the ND filter attenuates the laser. Then, HBT is performed on the source to measure the $g^{(2)}_{HBT}(0)$ value.

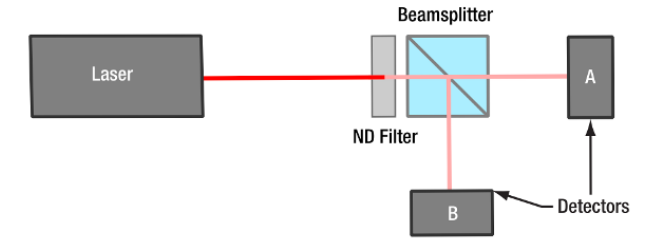

Figure 2.3: Schematic of the first experiment setup (Retrieved from: [3] Figure 111)

2.2.1 Procedure

The following steps were followed to set up the experiment:

1. After placing the alignment laser (making sure the beam is parallel to the table) on the left side, pointing to the right side, the beamsplitter was placed in front of it about 20 *cm* away. This beam splitter already has a Neutral Density filter attached to it.

2. Then, an alignment target, a fixed iris, was kept between them.

3. The alignment was done such that the center of the iris was kept in the middle of the laser, and then the reflection from the beamsplitter passed through the center of the iris.

4. Then, the first detector was placed 20 *cm* before the beamsplitter in the transmission path.

5. Now, I placed the alignment target between them. Then, the detector, attached to an economic beamsplitter, was aligned such that the laser spot was centered on the detector chip and the reflection from the economic beamsplitter passed through the iris.

6. The same was done again with the second detector in the reflection path.

7. Then, the detector optics were attached to the detectors and again slightly aligned to pass the reflection through the iris.

8. The detectors were connected to the time tagger, and the time tagger was connected to the pc.

9. Then, I checked the time tagger application's count rate to see each detector's count rate.

10. After this, the knobs on the detector optics were adjusted to make it such that I could see a get the maximum count rate.

11. After this, a zoom housing, part of the detector optics, was rotated to get to a point where I could see the maximum count rate.

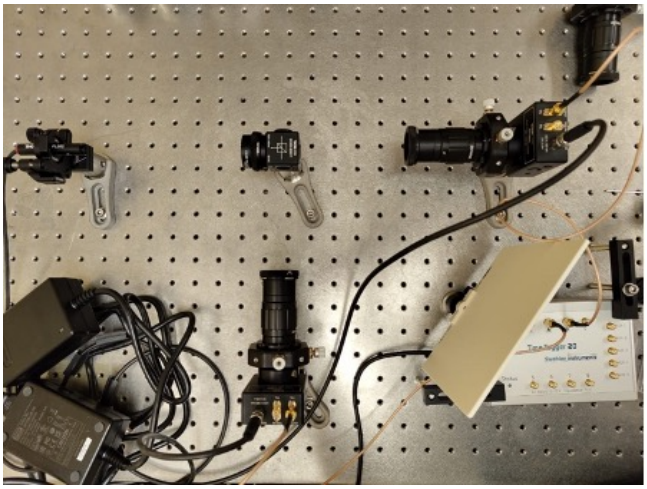

Figure 2.4: Image of the setup

2.2.2 Important Notes

The following are some points to be noted:

- The ND filter has an optical density of 3.0 which means, transmission is 0.1% (for 635 *nm*) [4].
- The beamsplitter has a 50 : 50 split ratio, AR coating, and non-polarizing. Even though these are the specifications, the beamsplitter is not precisely 50 : 50.
- The laser used has a wavelength of 635 *nm* with an output power of around 0.9 *mW*. But, the optical tube attached to the detectors has a bandpass filter [5] of central wavelength 810 *nm* and FWHM of 10 *nm*. It means that the laser wavelength lies outside of the bandpass filter. The transmission in the blocking region is $< 0.01\%$.
- After running some calculations to determine the final power on the detector, it is necessary to have this filter to reduce the power on the detector further and get as close to having one photon per interval case as possible. Higher power would cause too many photons to be present in one coincidence window.

- I have observed that any stray light greatly affects the readings, confirmed by Thorlabs technical support. However, they have never encountered a case where the light from the time tagger affects the reading. From my observations, the effect of the lights from the time tagger only affects longer run times.
- The time tagger has a dead time of 6 ns, so it doesn't take consecutive readings. Moreover, this time tagger doesn't keep a note of each time stamp for each coincidence. Instead, it counts the total number of coincidences over the integration time.
- If the laser was not left on for some time, weird fluctuations in the count rates for both A and B detectors. So, I recommend keeping the laser on for at least half an hour before measurements.

Figure 2.5: Observed fluctuations

2.3 Observations

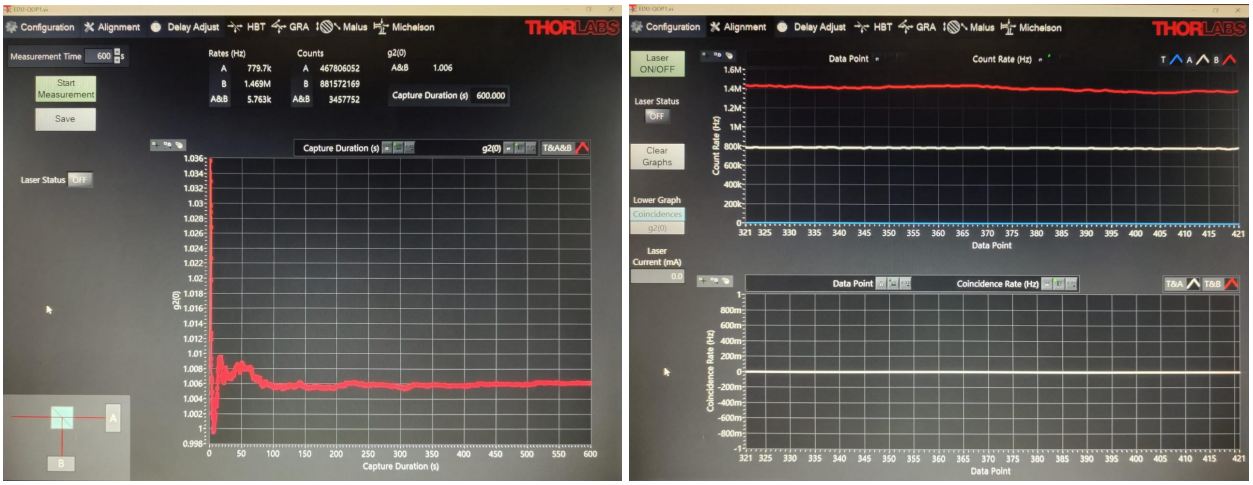

Figure 2.6: Left, plot of $g^{(2)}_{HBT}(0)$ for 600 s measurement time and 5 ns coincidence interval. Right, count rates of the detectors.

Figure 2.7: Left, plot of $g^{(2)}_{HBT}(0)$ for 900 s measurement time and 5 ns coincidence interval. Right, count rates of the detectors.

It can clearly be observed from fig. 2.6 and fig. 2.7 that the $g^{(2)}_{HBT}(0)$ value for both cases stagnate to 1, implying we have a coherent light source and not a quantum one.

2.3.1 Interpretation

We assume that the laser emits photons with a constant time interval and the photon energy matches the laser power. When the laser is attenuated by a factor of α, it doesn't mean that the photon energy reduces, but it means that every α^{th} photon passes through the filter. We can calculate the average number of photons n in a setup from the length l, speed of light c, and photon frequency f as follows:

$$n = \left(\frac{l}{c}\right) \cdot f$$

Given a setup length of 40 cm and a frequency of 2 MHz (from a 1 MHz average count rate at both detectors), we get:

$$n = \frac{0.4\ m}{c} \cdot (2 \times 10^6\ Hz) = 0.00266$$

It implies there are an average of 0.00266 photons in the setup, suggesting single photons that shouldn't split at the beamsplitter. They still result in $g^{(2)}_{HBT}(0) = 1$. However, this result indicates the assumption of evenly spaced photons is incorrect.
Laser light is represented by a coherent state with Poisson-distributed photon statistics. This inherent statistic does not change on reducing intensity, causing $g^{(2)}_{HBT}(0) = 1$ regardless of attenuation. Therefore, attenuated lasers can't perform single photon experiments due to unchanged underlying photon statistics.

2.4 Result

We have determined that an attenuated laser cannot be used as a quantum light source. It also checks that a laser is a coherent light source even when it is highly attenuated.

3 Experiment 2 (Generation of Photon Pair Source)

Aim: Generate a photon pair source and test whether the source emits photon pairs.

3.1 Theory

A photon pair source can be generated using a Spontaneous Parametric Down-Conversion (SPDC) and then detected using $g^{(2)}_{PS}(0)$ calculation. But here, the definition of $g^{(2)}_{PS}(0)$ is different from $g^{(2)}_{HBT}(0)$.

3.1.1 Spontaneous Parametric Down-Conversion (SPDC)

Spontaneous Parametric Down-Conversion (SPDC) [6] is a nonlinear optical process where a single photon (pump photon) interacts with a nonlinear crystal (like BBO) and splits into two lower-energy photons simultaneously. These photon pairs are correlated in various properties: time, polarization, momentum, and energy. It is the opposite of sum frequency generation. This process is purely quantum and cannot be explained classically.

There are two types of SPDC:

- Type 1 SPDC: Both photons have the same polarization.
- Type 2 SPDC: The photons have orthogonal polarizations.

Based on the phase-matching condition fulfilled and the type of SPDC, BBO crystals are of 2 types:

- Type 1 BBO: Produces photon pairs with identical polarizations, generally used for creating photon pairs without polarization entanglement.
- Type 2 BBO: Produces photon pairs with orthogonal polarizations, allowing for polarization entanglement.

The BBO crystal in this quantum optics kit is Type 1, which generates photon pairs but are not polarization-entangled pairs.

3.1.2 Correlation Function

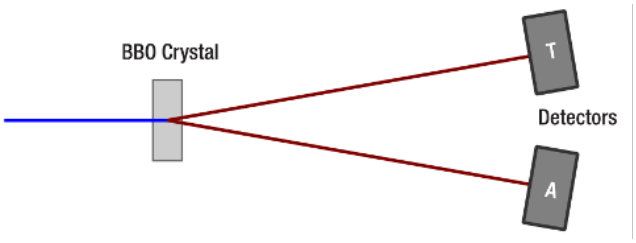

Figure 3.1: Schematic of the second experiment setup (Retrieved from: [3] Figure 112)

In the setup, there is no beamsplitter, so $g^{(2)}_{PS}(0)$ is different from the one in HBT.

$$g^{(2)}_{PS}(0) = \frac{R_{TA}}{R_T \cdot R_A \cdot \Delta t} \tag{10}$$

Here, R_T and R_A are the count rates of detectors T and A, respectively, R_{TA} is the coincidence count rate, and Δt is the coincidence window of the experiment.

In this definition, if there is a photon pair generation, they must reach the two detectors simultaneously, implying that there will be a very high coincidence rate. So, from eq. 10, $g^{(2)}_{PS}(0)$ should be very high, much greater than 1.

3.2 Experimental Setup and Procedure

In fig. 3.1, the laser is falling on the BBO crystal, undergoing SPDC, and, consequently, a photon pair is generated following two separate paths. Then, the detectors detect them and calculate $g^{(2)}_{PS}(0)$.

3.2.1 Procedure

The following steps were followed to set up the pump laser:

1. I assembled the pump laser, mounted it facing to the left and connected it to the laser diode controller.

2. Then I plugged everything, put a screen in front of the pump laser, and switched on the laser control box and the laser diode switch.

3. Then, I ensured that the polarity was set to "Cathode Grounded" and the maximum current was set to "50 mA".

4. After this, I wore the safety glasses, turned the key, and enabled the laser, which turned it on.

5. Now that the laser is on, there isn't any output because I haven't provided any input current. So, I slowly increase the current until it reaches the threshold value mentioned in the manual. At this point, the laser is now lasing. Before this, it was just fluorescing.

6. I adjusted the glass piece before the laser mount to collimate the beam as much as possible by checking the beam width at different distances. I checked at 20 cm, 30 cm, 50 cm, 80 cm, 1 m, 1.3 m, and 1.5 m using the screen.

7. In this setup, we have an iris aperture, which is kept directly in front of the laser mount to remove most of the stray light.

8. While setting up the laser, I noticed that the output from the laser was not parallel to the table. So, I used two mirrors to make the laser parallel in this process. I use the two-iris method to make sure the laser is parallel.

9. In this method, we have two iris apertures kept at a distance enough to cover the entire path length of the setup and adjust the two knobs of the mirrors such that the beam passes directly through precisely the middle of the two Iris apertures.

10. The first mirror adjusts the spot on the first iris, and the second mirror adjusts the spot on the second iris.

After this laser setup, I added an alignment laser and made it follow the same beam path as the previous laser using the same two iris apertures.
Note that we use a mirror with a magnetic mount that blocks the pump laser when placed and unblocks it when the mirror is removed. This way, once we have performed our rough alignment of the detectors with the alignment laser, we can remove the magnetic mirror mount and then use the pump laser to make further fine adjustments and take the readings.

Note: *We must also place a half-wave plate between the first two mirrors in the pump laser path, which is relevant when performing the fine adjustments. The orientation of the half-wave plate could be seen in fig. 3.2.*

The following are the images of the setup at this point :

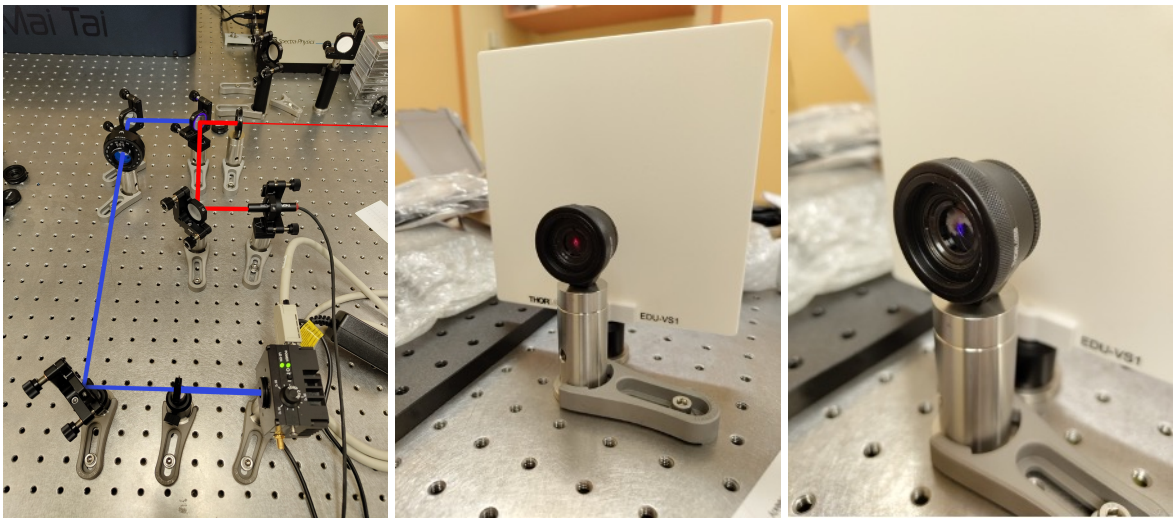

Figure 3.2: Left, beam path. Middle, spot made by alignment laser on the second iris. Right, spot made by pump laser on the second iris

For the next part, I attached the mirror and used the alignment laser. I put the screen between the two irises and the axicon closer to the first. Note that the axicon mount is also magnetically attached and can be switched for the fluorescence filter or the BBO crystal without changing the position of the post.

I adjusted the axicon so that the laser passed through its center. To ensure its plane was perpendicular to the laser, I used the alignment target (a fixed iris on stiff paper). The alignment was done so that

the reflection from the axicon passed again through the iris on the alignment target. This alignment was also done while seeing the output on the screen, which should be an even circle. At first, it wasn't even a circle, but as I aligned it better, it became an even circle. It was a lot of hit and trial, but it worked after a while.

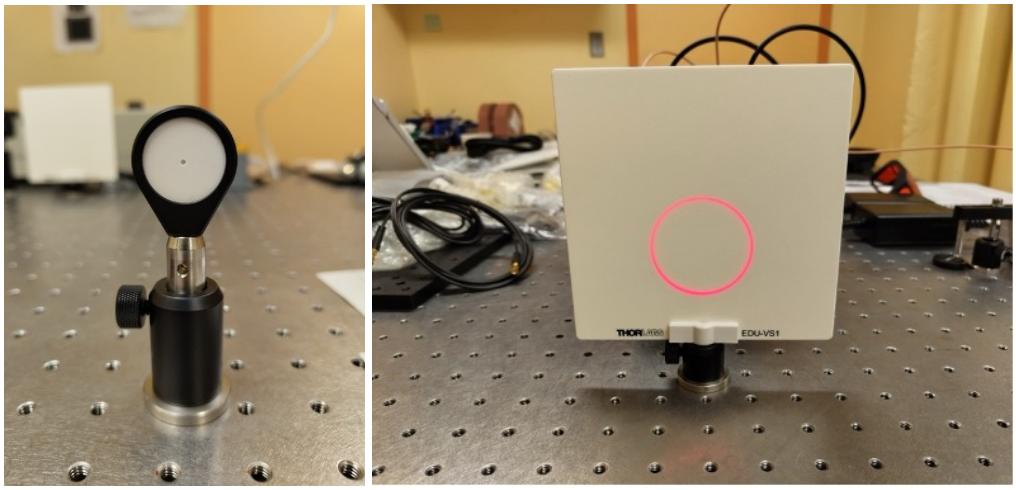

Figure 3.3: Left, alignment target. Right, the circle formed due to the axicon

It is to be noted that I first made sure the height of the alignment target was the same as the other two iris, and the second iris also acts as a beam block for the system when we close its lid.

After doing this, we can remove the screen, so I placed the detectors, as you can see below.

Working with one detector at a time, first, we remove the detector optics and replace it with an economic beamsplitter, and then we place the alignment target in front of the detector, such that the spot from the target falls on the middle of the detector and their reflection from the economic beamsplitter goes through the alignment target again. I did this again for the second detector after ensuring they were almost symmetrical and equally distanced. I then put back the detector optics.

Before starting the next part, we would connect the detectors and switch on the time tagger application on the PC to monitor the count rates on the detector.

After this, I removed the magnetic mirror attachment and switched on the pump laser at 19.5 mA, which is around 5 mA below the threshold current of this laser.

After this, I removed the axicon and put the fluorescent filter in place. Now, the light going through the fluorescent filter will fluoresce onto the detector. And so now we can make the fine adjustments to the detectors. I opened the first Iris aperture entirely and let the maximum light fall onto the detectors.

Then, I put the zoom housing of the detector optics in the middle and adjusted the XY axis of the detective optics. For this, I first tried to reach a maximum on the X-axis and then on the Y-axis. Then I adjusted the zoom housing so that I hit a maximum and then adjusted the XY again and repeated

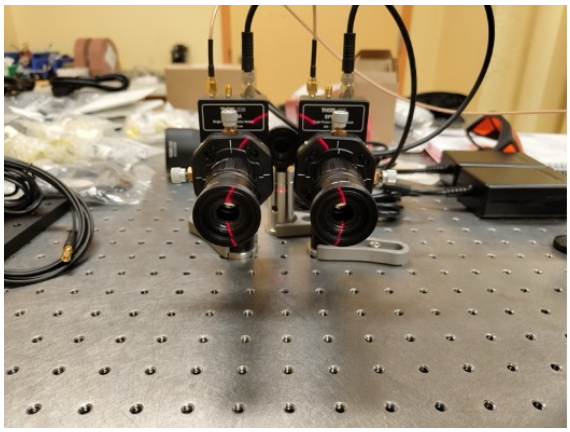

Figure 3.4: This is how the alignment looks before removing the magnetic mirror attachment.

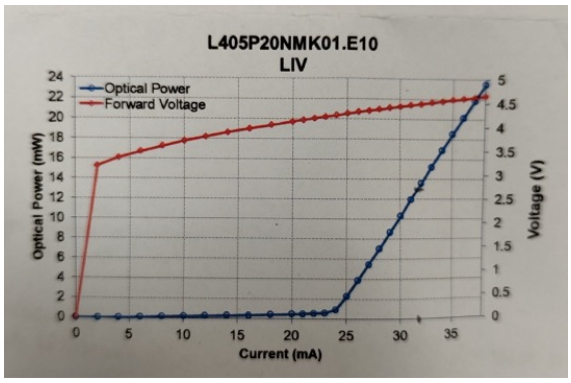

Figure 3.5: Plot of optical power vs. current plot for the laser provided by Thorlabs

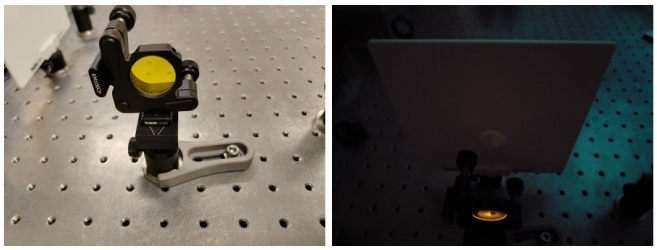

Figure 3.6: Fluorescent filter and its output on screen

this whole procedure till I finally reached the maximum and couldn't do better. I repeated the same exercise for the second detector and ensured that the output on the time tagger application was at least around 300k count rate.

After this was done, I switched the fluorescent filter out for the BBO crystal and slowly increased the power of the laser to 32 mA. It is to reach the output power of 13 mW (fig. 3.5).

At this point, the laser is in its lasing mode, and now we should be able to have a quantum light source that is falling onto the detectors. Now fine adjustments can be made again by adjusting the lower screws on each of the detectors such that we get as much count rate as possible.

We need to close the time tagger application and switch to the main application for this setup to check if we have a quantum light source. The coincidence window was then set to 20 ns, and the

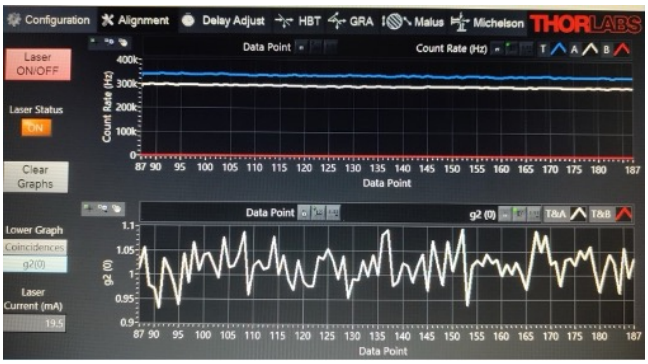

Figure 3.7: The count rates higher than or equal to $300k$ and the $g^{(2)}_{PS}(0)$ value is close to 1, so we still don't have a pair of photons generated.

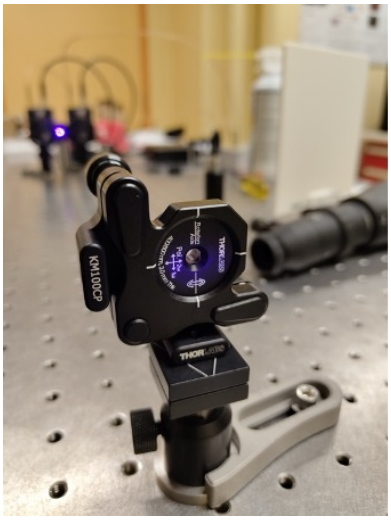

Figure 3.8: The BBO crystal mount on the path of the pump laser

coincidences and the count rates were measured. The software used this to calculate the $g^{(2)}_{PS}(0)$, the second-order correlation function. We should have an extremely high $g^{(2)}_{PS}(0)$ value in this scenario. It is because if we generate a pair of photons, they must be incident onto the detector at the same time most of the time. If this happens, the coincidences will be much more than a completely uncorrelated or weakly correlated system. Since the coincidences are not random and the photons are correlated to each other, the $g^{(2)}_{PS}(0)$ shoots up very high, and as we can see in this image, it is around 200.

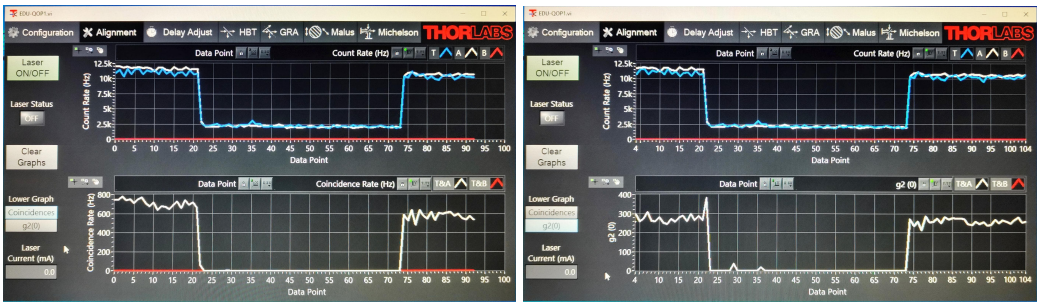

Figure 3.9: Left, the plot with coincidence count rate. Right, the plot with $g^{(2)}_{PS}(0)$

The dip you can see is when I blocked the source, proving this result is not because of background noise but because of the photon pair generated by the light from the BBO crystal.

Note: *If we do not see the $g^{(2)}_{PS}(0)$ value very high or, let's say, around 1, then there could be a case that the detectors are not equally distanced from the BBO crystal, and so we would need to align it again so that it is equally distanced. Then, I used the half-wave plate and adjusted its angle to get to a maximum.*

After this, the manual says to perform a delay adjustment, which is used to ensure that the detectors have a delay between them to get the highest coincidence count rates. The manual says to set the A to T delay based on the central maxima we see here, which I did. It is done to finely adjust the path length such that we get a delay between paths equal to 0.

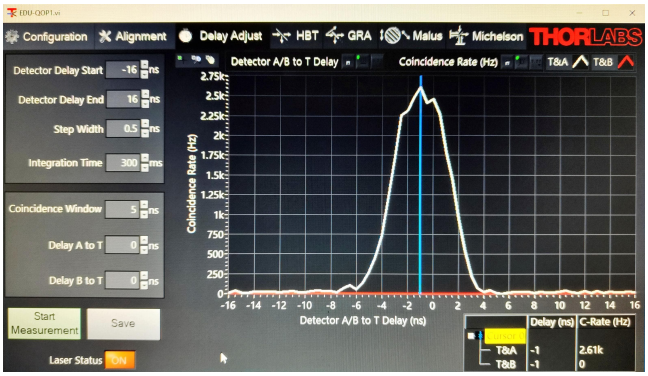

Figure 3.10: Plot of coincidence rate vs. delay

3.2.2 Important Notes

The following are some points to be noted:

- I attached a power meter probe and aligned it correctly and directly in front of the laser. After this, I slowly increased the power of the laser from 0 *mA* to 42 *mA* with increments of 0.5 *mA* while giving at least 1-2 minutes between each reading, letting the system stabilize before each reading. I could plot the following graph.

  Comparing this plot to the fig. 3.5, you can see that the plot is shifted, but the trend remains the same. It might not always be the case, but it is possible that the laser does not show the exact plot as the specification sheet.

- I re-aligned everything again and again. The procedures were mostly the same as earlier. One thing to note is that after putting the BBO crystal, you can adjust the knobs of the BBO mount to get to a maximum. I found that we can also use the app to see which point the detectors have a maximum count rate. It is slightly different from the manual because it only tells us to align the BBO so that the reflection from it passes again through the alignment laser, i.e., precisely in line with the laser. However, the alignment with the fluorescent filter seems different from the BBO, making things more complicated.

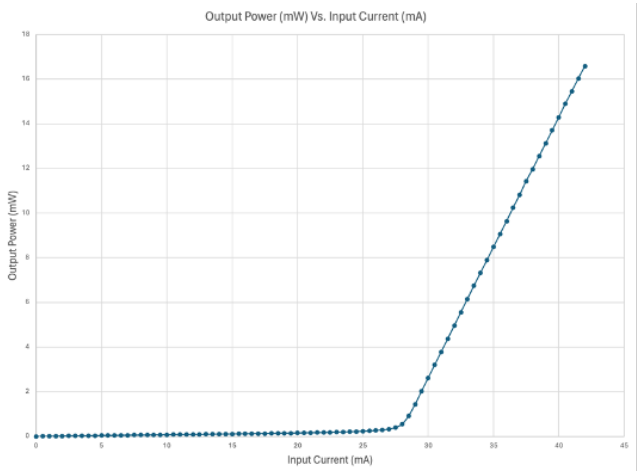

Figure 3.11: Observed optical power vs. current plot for the laser

- Before this, while aligning with the fluorescence filter, I couldn't get more than 300 KHz count rate on one of the detectors, but after the re-alignments, I was able to get more than that on both detectors. But this didn't improve the count rate with BBO by that much immediately, so after putting the BBO, I had to adjust the knobs on the BBO crystal and slightly adjust the detector knobs to improve.

Figure 3.12: Count rates of both detectors after re-alignment

- After ensuring these things were all in place, I took the following readings, which I compiled in graph form.
  As you can see from these plots:
  1. There is a linear increase in count rates with input current, which aligns with fig. 3.11.
  2. The coincidence count rates are maximum at around 36 mA.
  3. However, the $g^{(2)}_{PS}(0)$ keeps reducing as the current increases to around 84 at 36 mA current.
  4. Meanwhile, $g^{(2)}_{PS}(0)$ is around 171 at 32 mA.
  5. But as you can see, at no point does it go past even 5.5k, so I don't think I will be able to get a better coincidence count rate.
  6. So, I will work with 32 mA but increase or decrease the input current based on whether I need more count rate.

- As you can see in fig. 3.14, the fluorescent filter is a long-pass filter at 515 nm, meaning the incoming laser, which is at 405 nm, will only have its 515 nm and above component transmit. Since Thorlabs doesn't mention any angles, so I assume it is simply a colored glass long-pass filter that

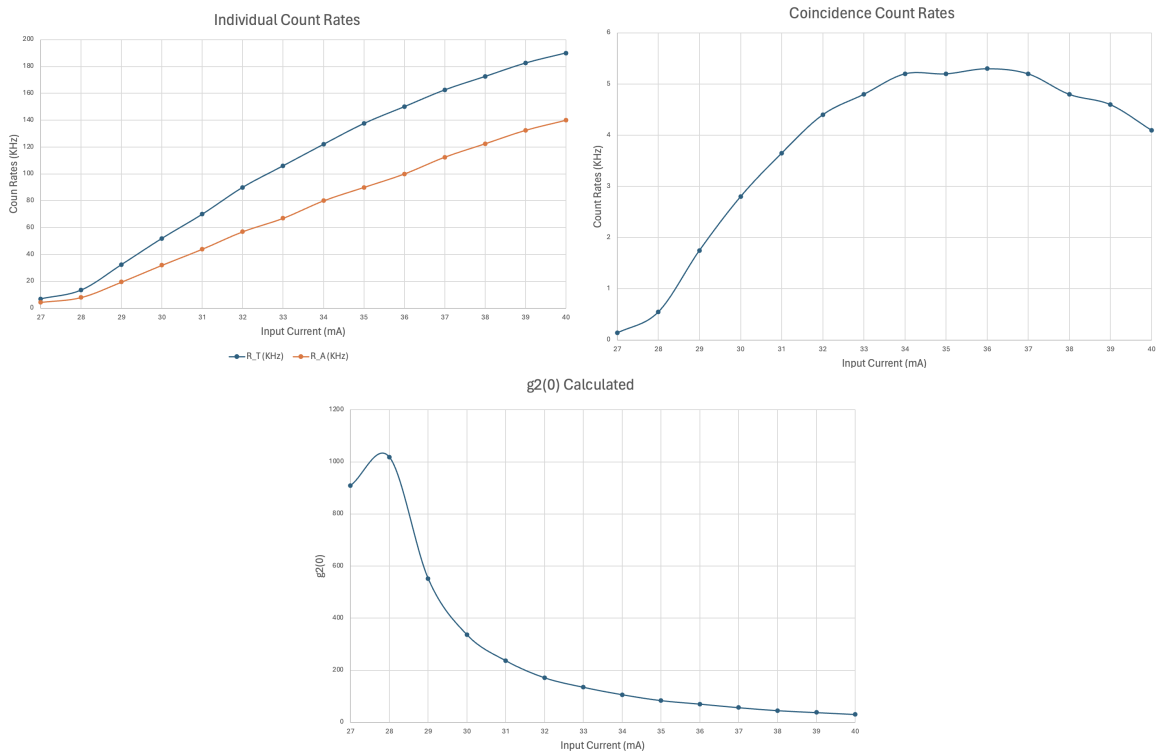

Figure 3.13: First, individual count rates vs. input current. Second, coincidence count rates vs. input current. Third, $g^{(2)}_{PS}(0)$ calculated vs. input current

blocks out the central wavelength and lets the rest fluoresce at the detector. That is why the color of the light after the fluorescent filter is not blue, and the intensity is lesser [7].

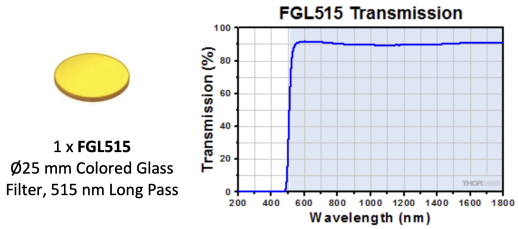

Figure 3.14: Fluorescent filter specifications (Retrieved from: [3][7])

3.3 Observations

You can see the plots in fig. 3.15, but note that this still doesn't have good enough count rates. The count rates could still be way higher. I have reduced the coincidence window to 5 *ns*, which is more relevant in the context of this experiment.

This adds up as:
Coincidence count rate is around $3.2k$.
The count rate of T is around 57500.
the count rate of A is around 55000.
Coincidence window is 5 *ns*.

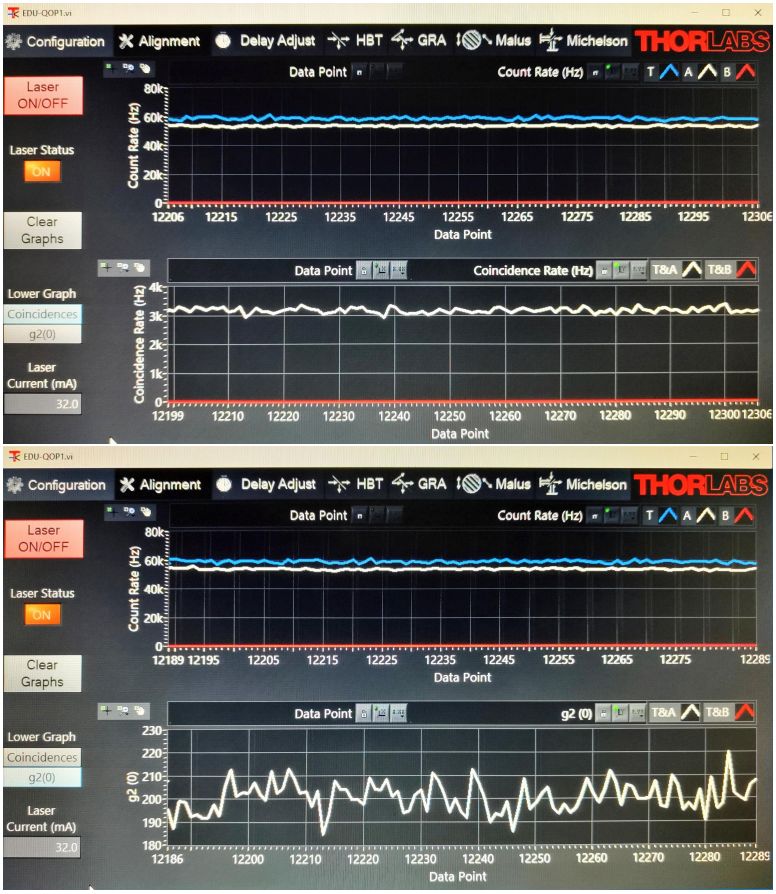

Figure 3.15: First, coincidence count rate. Second, $g^{(2)}_{PS}(0)$.

So,

$$g^{(2)}_{PS}(0) = \frac{3200}{(57500 * 55000 * 5 * 10^{-9})} = 202.37$$

Which is what we observe.

In fig. 3.16, I have changed the coincidence rate from 5 *ns* to 1 *ns*. Doing this seems to have increased the $g^{(2)}_{PS}(0)$ value even though the coincidence count rate has lowered.

This happens because even though I have reduced the coincidence time by 5 times, the coincidence count rate has only been reduced by around three times. So, overall, there is an increase of around $5/3$ times, which, starting from 170 at 5 *ns* coincidence window, leads to around 283 $(= 170 * 5/3)$, which is what we see here.

3.3.1 Interpretation

Generation of photon pair source:

- The polarization of the pump laser is perpendicular to the optical table's plane.
- The half-wave plate, set at 45°, rotates the polarization of the pump beam to lie parallel to the table plane.

Figure 3.16: First, coincidence count rate. Second, $g^{(2)}_{PS}(0)$.

- The BBO crystal is oriented with its optical axis parallel to the table plane as shown in fig. 3.17.
- The axis of rotation of the crystal, which is adjusted for phase matching, is perpendicular to the table.
- Then the polarizations of the signal and idler photons coming out of the crystal will be perpendicular to the plane of the table which is the same parallel to the axis of rotation.
- The polarization of the photon pair remains perpendicular to the table plane.

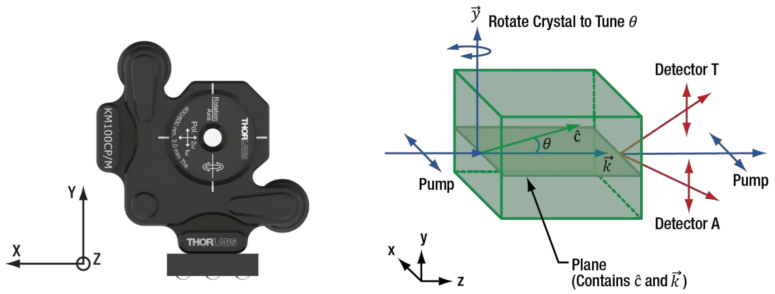

Figure 3.17: Photon pair generation using SPDC (Retrieved from: [3] Figure 161)

From section 3.3, it is clear that the two paths have a very high correlation, which aligns with the description of photon pair generation through SPDC. The polarization mentioned in fig. 3.17 can be

checked by keeping a polarizer in front of one of the detectors and checking the count rates at 0° and 90°.

3.4 Result

We have generated a photon pair source using SPDC. They have a very high correlation, and using that fact, we have also tested that the source does emit photon pairs.

4 Experiment 3

Aim: Test whether one arm of the photon pair source can serve as a single-photon source.

4.1 Experimental Setup and Procedure

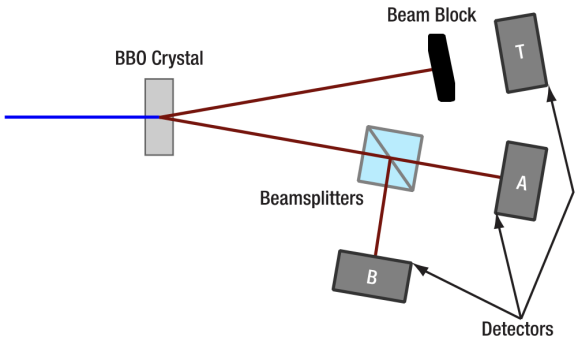

Figure 4.1: Schematic of the third experiment setup (Retrieved from: [3] Figure 113)

4.1.1 Procedure

The following steps were taken to set up the third detector:

1. I first switched off the pump laser.
2. Then, I replaced the BBO crystal with the axicon and attached the magnetic mirror mount to enable the alignment laser. So, then, I turned on the alignment laser.
3. I placed the alignment target in the left beam path.
   Note: *The manual says to place the beamsplitter on the right path, but I placed it in the left path because I saw higher count rates on that side.*
4. Then I placed the beamsplitter with the attached iris aperture about 10 breadboard holes in front of the left detector (iris facing the alignment target). I made sure that the light passing through the target was centered on the iris of the beamsplitter.
   Note: *I removed the ND filter from the beam splitter used in the first experiment.*
5. Then I rotated the beamsplitter until the reflection from the beamsplitter passed back through the hole in the alignment target.
6. I fixed the beamsplitter, making sure the laser was still aligned at its center.
7. Then, I placed the third detector (equipped with the economic beamsplitter) on the reflection part of the beamsplitter, the same distance away as the detector on the transmission side.
8. I put the alignment target between the third detector and the beamsplitter, such that the light from the beamsplitter reflection passed through the center of the alignment target.

9. I aligned the detector such that the beam from the alignment target was centered on the detector chip and the reflection from the economic beamsplitter passed back through the center hole of the alignment target.
   Note: *For this part, I had attached the economic beamsplitter on the detector instead of the detector optics. So, there were two reflections from the detector. One was from the economic beam splitter and one slightly diffused was coming from the detector chip. The reflection that should pass through the center of the alignment target is the one from the economic beamsplitter and not the one that bounces from the detector chip.*

10. Then I just fixed the detector, put the detector optics instead of the economic beamsplitter, and again ensured everything was aligned correctly.

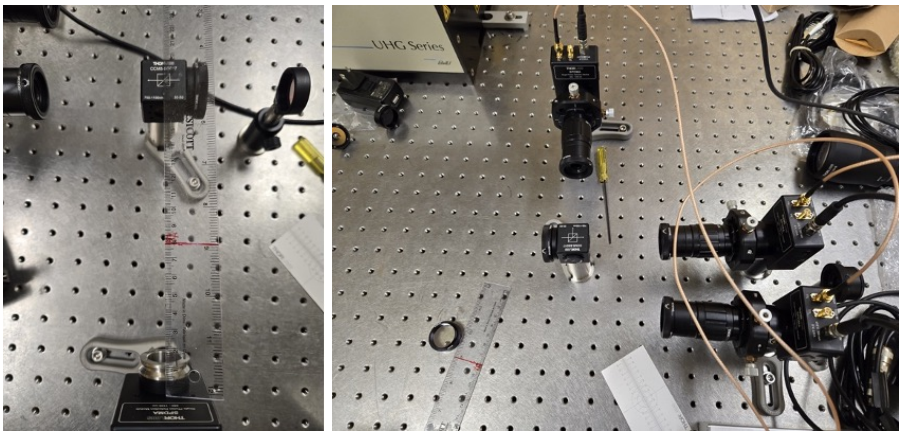

Figure 4.2: Shows the detector alignment at this point.

After this, I followed the same procedure as experiment 2 for the fine adjustment, first with the fluorescent filter, then the BBO, and then the delay adjustment.

4.1.2 Important Notes

The following are some points to be noted:

- The beam splitter is not precisely 50 : 50 as mentioned in section 2.2.2, so the count rates measured will not be completely equal.

- Till this point, I had a lot of issues with the pump laser, like the lack of power from it, the beam not being properly collimated, and observing some major fringes on the laser spot. While going through the Thorlabs website to figure out what might be wrong, I realized that there was something wrong with the orientation of the lens. It turned out that the assembly mentioned in the manual PDF was incorrect. They provided an extra page with the corrections separately in the physical manual but not in the PDF, and I followed the PDF manual from the beginning.
  Note: *After mentioning this to Thorlabs, they have now corrected the mistake from the PDF, which is available on their website [3].*

After fixing the lens orientation, the laser had almost no fringes, and the beam spot was way more collimated and intense. I had taken some readings for experiments 3, 4, and 5 before this change, but they were not that good since you need a good amount of count rates. So, the observations I will show now are from this fixed pump laser.

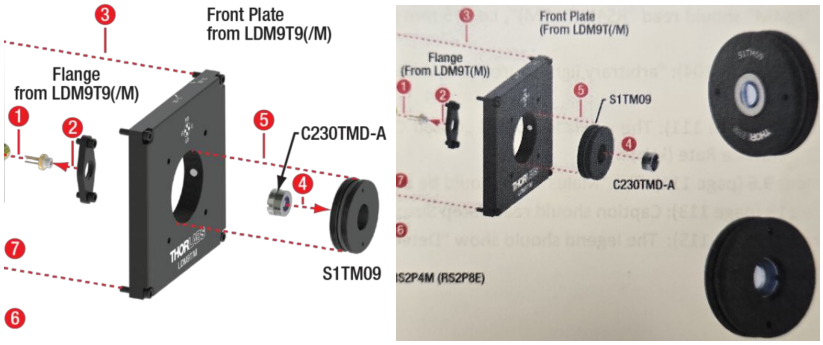

Figure 4.3: Left, the orientation of C230TMD-A in the PDF. Right, the correction page of the manual (Image source: [3] Figure 27)

The following are the new count rates, coincidence rates, and $g^{(2)}_{PS}(0)$ with the fluorescence filter and the BBO crystal:

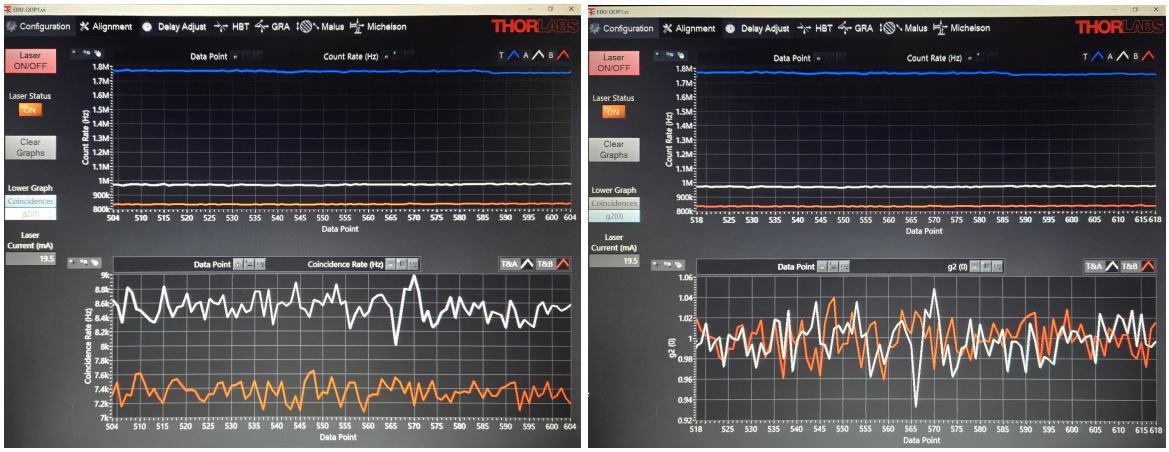

Figure 4.4: Left, coincidence count rate. Right, $g^{(2)}_{PS}(0)$

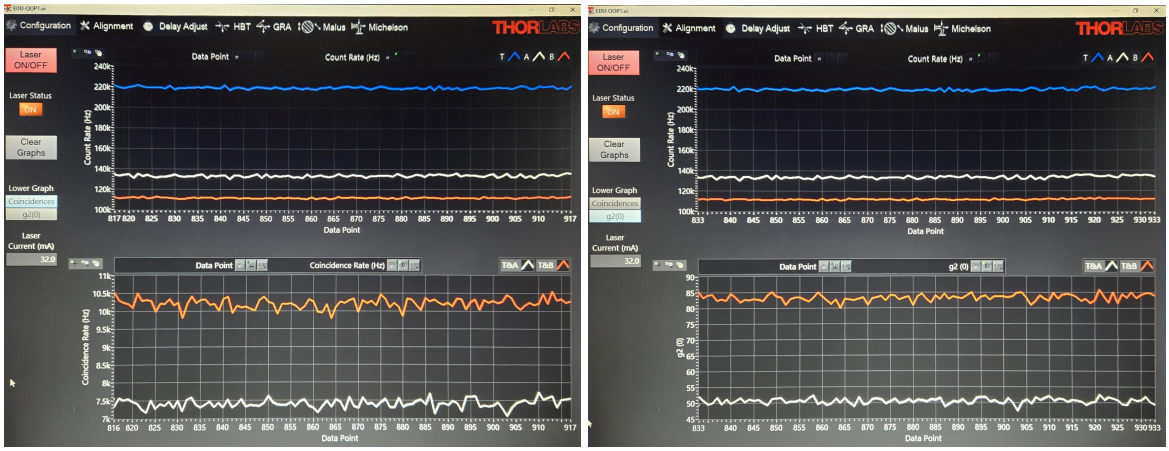

Figure 4.5: Left, coincidence count rate. Right, $g^{(2)}_{PS}(0)$

As you can see, the coincidence count rate for BBO crystal, even 32 mA input current, is above 10 KHz, at least for the T&B coincidence. The other one is smaller but still way better than before.

4.2 Observations

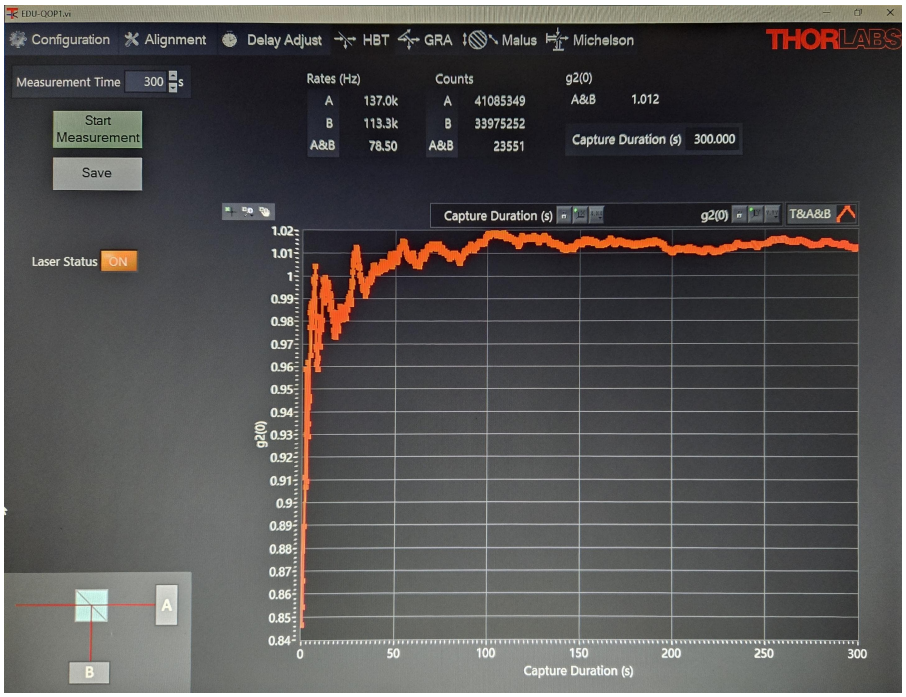

Figure 4.6: Plot of $g^{(2)}_{HBT}(0)$ for 300 s measurement time and 5 ns coincidence interval

Fig. 4.6 is the result of the HBT experiment performed on only one of the arms of the photon pair source.

4.2.1 Interpretation

In this experiment, we see that even though we have a photon pair source, which is a single photon source, we still see classical behavior if we only look at one of the two arms of the pair source. It is happening because the quantum nature of the pair source is the generation of simultaneous photon pairs, which is why they are called correlated, but when we only consider one of the two photons, there is no correlation. Let's consider a trail of photons coming into the BBO crystal as a coherent state. While the photon pairs are emitted from the BBO crystal, photons in the individual arms will follow a thermal state (classical light source). But as mentioned at the end of section 2.1.2, the kit displays it as a coherent state, meaning $g^{(2)}_{HBT}(0) = 1$.

4.3 Result

We have shown that one arm of the photon pair source is classical in nature and, so, can not be used as a single photon source.

5 Experiment 4 (Grangier-Roger-Aspect Experiment)

Aim: Test whether the pair source can serve a single-photon source when counts are considered in coincidence with the trigger detector.

5.1 Theory

Grangier-Roger-Aspect (GRA) [8] experiment is used to determine the nature of light source when we have a pair source or, say, two output sources that may or may not be related to each other. For this kit, the setup used for this experiment is shown in fig. 5.1.

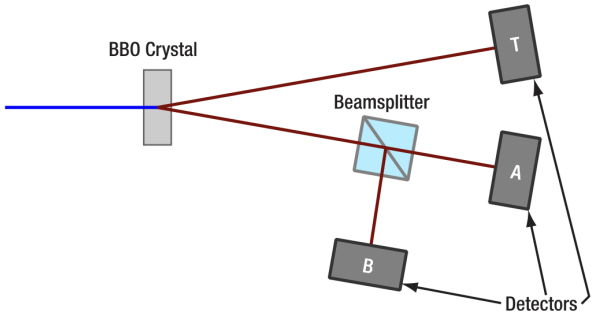

Figure 5.1: Schematic of the GRA experiment (Retrieved from: [3] Figure 114)

5.1.1 Correlation Function for GRA experiment

In this scheme, instead of measuring the probability of photons reaching each detector, the probability of coincidences is measured. P_{TA}, P_{TB}, and P_{AB} are the probabilities of observing coincidences in detectors T-A, T-B, and A-B respectively. P_{TAB} is the probability of observing a triple coincidence. T is the detector with no beamsplitter in the path and is called the trigger detector. So, basically, we measure the coincidences whenever there is a detection at detector T. The expression of $g^{(2)}_{GRA}(0)$ similar to eq. 7 in terms of the coincidence probabilities is given by:

$$g^{(2)}(0) = \frac{P_{TAB}}{P_{TA} \cdot P_{TB}} \tag{11}$$

The probabilities in the triple coincidence case can be normalized to the count rate of the trigger detector T, as this is the maximum rate of counts at the other detectors.

$$P_{TA} = \frac{R_{TA}}{R_T} \qquad P_{TB} = \frac{R_{TB}}{R_T} \qquad P_{TAB} = \frac{R_{TAB}}{R_T} \tag{12}$$

Substituting these in eq. 11 gives,

$$g^{(2)}(0) = \frac{R_{TAB} \cdot R_T}{R_{TA} \cdot R_{TB}} \tag{13}$$

5.1.2 Triple Coincidence Scheme

The kit uses a scheme known as the coincidence of coincidence scheme to determine triple coincidences.

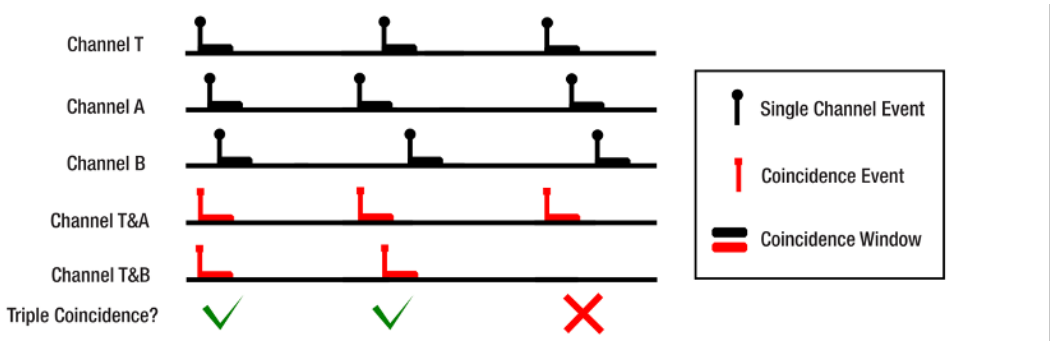

Figure 5.2: Shows some cases of coincidence of coincidence scheme (Retrieved from: [3] Figure 20)

In fig. 5.2, the first and second cases result in a triple coincidence. This happens due to the coincidence of coincidence (CC) scheme [3]. In the first case, events on channels T, A, and B occur within each other's coincidence windows, leading to registered coincidences between $T\&A$ and $T\&B$, resulting in a triple coincidence. In the second case, although events on A and B do not coincide directly with each other, the time tagger still registers a triple coincidence because both $T\&A$ and $T\&B$ have their respective coincidence events within the coincidence window of T. It shows that the CC scheme relies on coincidences between the trigger detector (T) and each of the other two detectors (A and B), rather than requiring a direct coincidence between A and B. In the third case, although T and A coincide, B does not fall within the coincidence window of T, so no triple coincidence is recorded.

5.2 Observations

Figure 5.3: Plot of $g^{(2)}_{GRA}(0)$ for 60 s measurement time and 5 ns coincidence interval.

There are no setup changes from the previous experiment, so the setup remains the same. Fig. 5.3 is the result of the GRA experiment showing that the $g^{(2)}_{GRA}(0) = 0.03$ which is much less that 1.

5.2.1 Interpretation

In this experiment, we see that when we consider both the arms of the pair source together, we can finally see the anti-correlation, which is the quantum behavior. This is because when we consider the triple coincidence scheme, it is obvious that if we have one of the photon pairs reach the detector T, then at the same time, we can only have a photon at either detector A or B. We cannot have a signal at both because a photon will either reflect or transmit and not split at the beamsplitter. It means that the probability of triple coincidence (P_{TAB}) should be 0. So, we observe $g^{(2)}_{GRA}(0) < 1$ which means we have a quantum source.

5.3 Result

We have shown that the photon pair source, when considered together, is quantum in nature and, so, is indeed a single photon source.

6 Experiment 5

Aim: Perform the GRA experiment with a classical source.

6.1 Observations

In this experiment, I simply magnetically attached the fluorescent filter instead of the BBO and adjusted the current accordingly, as mentioned before.

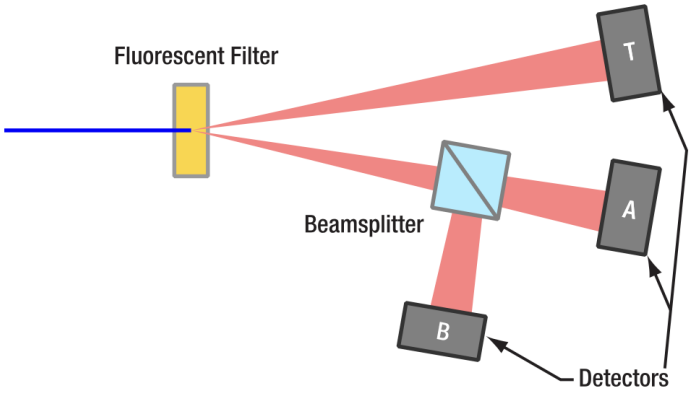

Figure 6.1: Schematic of the GRA experiment with classical light (Retrieved from: [3] Figure 115)

Fig. 6.2 is the result of the GRA experiment performed on the light from fluorescent filter showing that the $g^{(2)}_{GRA}(0) = 1$.

Figure 6.2: Plot of $g^{(2)}_{GRA}(0)$ for 60 s measurement time and 5 ns coincidence interval.

6.1.1 Interpretation

In this experiment, when we use a classical light, the GRA experiment does show $g^{(2)}_{GRA}(0) = 1$ as there are only random coincidences and no correlation. It is done to demonstrate that the reason for

detecting the quantum source is not just because we used a triple coincidence detection scheme. The more important aspect is the source used.

Note: *The light from the fluorescent filter is actually a thermal state, but due to the same reason mentioned at the end of section 2.1.2, we see* $g^{(2)}_{GRA}(0) = 1$.

6.2 Result

We performed the GRA experiment with a classical source and confirmed that the detection scheme is indeed able to differentiate between classical and quantum light sources.

7 Experiment 6

Aim: Test the polarization properties of single photons.

7.1 Theory

Malus' law [9] describes how the intensity of light varies when passing through a polarizer at various polarization angles.
This relation is known to follow a cos-squared function. The following is the expression:

$$I(\theta) = I_0 \cdot cos^2(\theta) \tag{14}$$

Here, if θ_1 is the polarization angle of the incoming light and θ_2 is the polarization angle of the polarizer, then $\theta = \theta_2 - \theta_1$, meaning θ is the angle of the polarizer with respect to that of the light. I_0 is the intensity of incoming light, and $I(\theta)$ is the intensity of the light after the polarizer, which is a function of θ.

7.2 Experimental Setup and Procedure

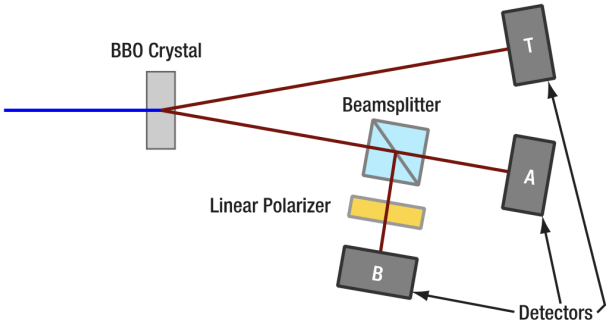

Figure 7.1: Schematic of the experiment 6 setup (Retrieved from: [3] Figure 116)

7.2.1 Procedure

The following steps were followed to calibrate the polarizer:

1. I kept the polarizer, laser pointer, and screen in a linear configuration (see fig. 7.2).
2. Then I adjusted the dial of the polarizer to see a minimum intensity spot and noted the angle (see fig. 7.3).
3. Then, I flipped the polarizer, did the same to see a minimum spot, and noted the angle.
4. Finally, I took the angle which is in between the two minimums, loosened the two screws of the dial, adjusted the dial so that the 0° is with the 0, and then tightened it up again.

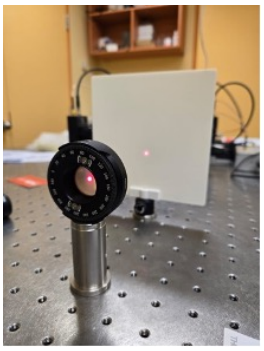

Figure 7.2: Linear configuration of the optics

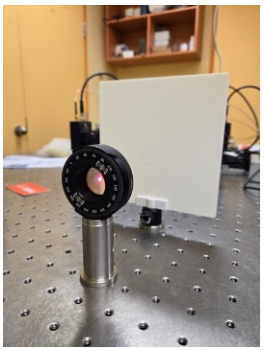

Figure 7.3: Minimum spot

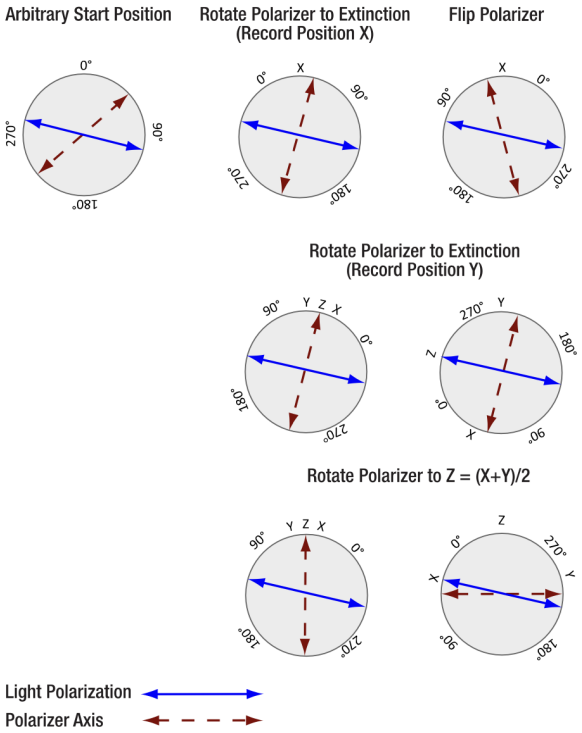

Figure 7.4: Schematic for the procedure to calibrate the polarizer (Retrieved from: [3] Figure 64)

After this, I placed the Ø1.0" polarizer in front of Detector B and ensured that it was centered using the reflection on the Alignment target as I have done in all the previous experiments. After that, I locked the polarizer's base and took the readings.

For taking the readings, I kept the time for each measurement to be 20 s and went from 0° to 360° by rotating the polarizer dial with increments of 10° for each measurement.

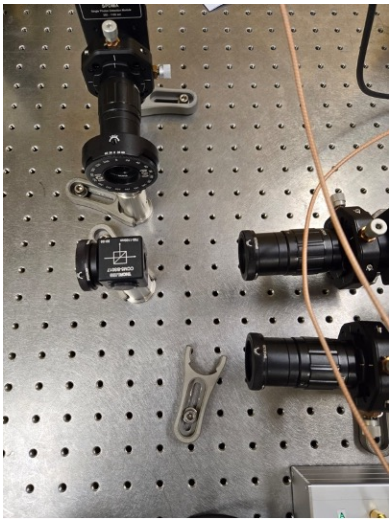

Figure 7.5: Setup of experiment 6

7.2.2 Important Notes

The following are some points to be noted:

- When I first started to perform the experiment with the Ø1.0" polarizer, I saw an asymmetric graph.

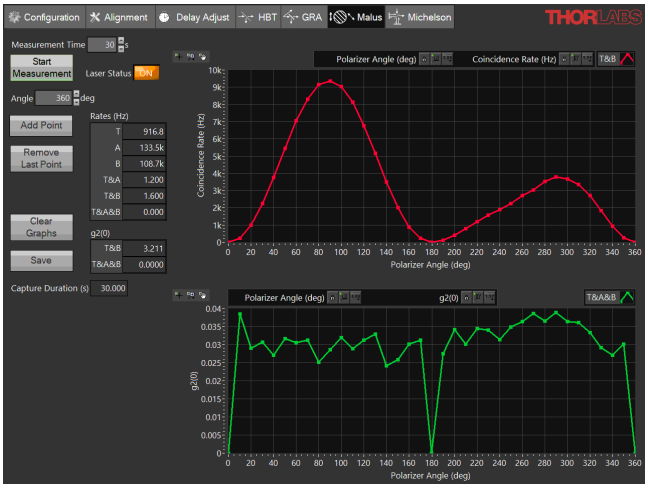

Figure 7.6: T-B coincidence rate vs. relative polarizer angle

As you can see from fig. 7.6, even though the 0 values are at the correct angles, one side is higher than the other. I ensured the polarizer was correctly attached, but the problem persisted. So, I suspected that there must be a problem with the polarizer and swapped it for the Ø1/2" polarizer (given for the Quantum Eraser experiment). This polarizer worked properly.

- The $g^{(2)}_{GRA}(0)$ values at 0°, 180°, and 360° are 0 in my case because the coincidence count rates at that point are so low that there was no triple coincidence at all. This is different from the Thorlabs manual as they show an abnormally high $g^{(2)}_{GRA}(0)$ value at those angles because, in their case, the detectors probably detected a few triple coincidences while having a very low coincidence count rate. We anyways discard those data points for $g^{(2)}_{GRA}(0)$ because they are very unreliable and inconsistent.

7.3 Observations

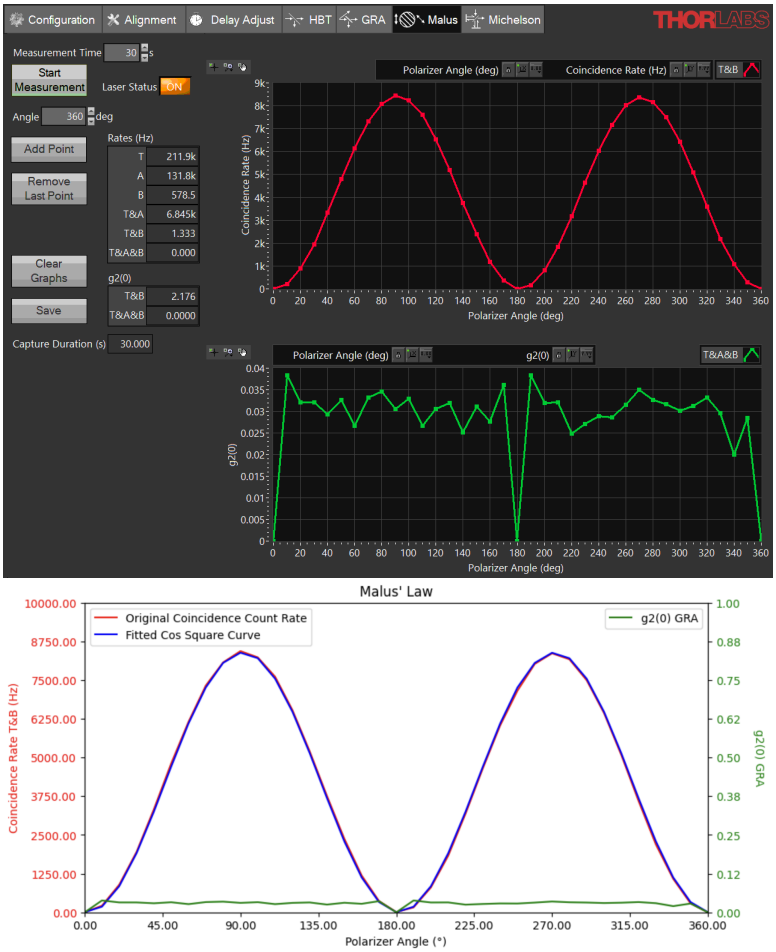

Figure 7.7: Graphs observed and plotted for the Malus' law experiment on quantum light

As you can see, the data received in the experiment perfectly with the cos-squared curve while having the g2(0) < 1 the entire time.

7.3.1 Interpretation

The reason why it still works is that when going from classical to quantum is because a quantity like transmission from the beamsplitter is replaced by their respective probabilities, and the coincidence rate would be proportional to the transmission probability and the transmission intensity. The same

is also true for reflection.

$$R_{TB} = R_{TB}^{max} \cdot cos^2(\theta) \tag{15}$$

Here, R_{TA} is the coincidence count rate of detectors $T\&B$, R_{TB}^{max} is the maximum coincidence count rate of detectors $T\&B$, and since we set the 0° polarization of the polarizer to be in the plane of the table (perpendicular to the polarization of photon pairs), $\theta = \theta_2 + 90^\circ - \theta_1$.

7.4 Result

We tested the polarization properties of single photons and determined that even though we are working with a photon pair source, we still see classical wave phenomena like Malus' Law.

8 References

1. Thorlabs. *EDU-QOP1 Software* https://www.thorlabs.com/software_pages/ViewSoftwarePage.cfm?Code=EDU-QOP1.
2. Brown, R. H. & Twiss, R. Q. Correlation between Photons in two Coherent Beams of Light. *Nature 1956 177:4497* **177,** 27–29. ISSN: 1476-4687. doi:10.1038/177027a0 (4497 1956).
3. Thorlabs. EDU-QOP1(/M) Quantum Optics Kit User Guide. https://www.thorlabs.com/_sd.cfm?fileName=MTN036012-D02.pdf&partNumber=EDU-QOP1.
4. Thorlabs. *Thorlabs - NE30A Ø25 mm Absorptive ND Filter* https://www.thorlabs.com/thorproduct.cfm?partnumber=NE30A.
5. Thorlabs. *Thorlabs - FB810-10 Ø1" Bandpass Filter* Thorlabs. https://www.thorlabs.com/thorproduct.cfm?partnumber=FB810-10.
6. Burnham, D. C. & Weinberg, D. L. Observation of Simultaneity in Parametric Production of Optical Photon Pairs. *Physical Review Letters* **25,** 84–87. ISSN: 00319007. doi:10.1103/PhysRevLett.25.84 (2 1970).
7. Thorlabs. *Thorlabs - FGL515 Ø25 mm Colored Glass Filter* Thorlabs. https://www.thorlabs.com/thorproduct.cfm?partnumber=FGL515.
8. Grangier, P., Roger, G. & Aspect, A. Experimental Evidence for a Photon Anticorrelation Effect on a Beam Splitter: A New Light on Single-Photon Interferences. *Europhysics Letters* **1,** 173. ISSN: 0295-5075. doi:10.1209/0295-5075/1/4/004 (4 1986).
9. Hecht, E. Optics, Fifth Edition. *Pearson Education Limited* (2017).